# Total gaseous mercury emissions from soil in Guiyang, Guizhou, China

Xinbin Feng

State Key Laboratory of Environmental Geochemistry, Institute of Geochemistry, Chinese Academy of Sciences, Guiyang, China

Shaofeng Wang, Guangle Qiu, Yamin Hou, and Shunlin Tang

State Key Laboratory of Environmental Geochemistry, Institute of Geochemistry, Chinese Academy of Sciences, Guiyang, China

Graduate School, Chinese Academy of Sciences, Beijing, China

Received 30 November 2004; revised 4 April 2005; accepted 15 April 2005; published 26 July 2005.

[1] Guiyang is located in the Circum-Pacific Global Mercuriferous Belt, and mercury concentrations in soil in this area are enriched. In situ total gaseous mercury (TGM) exchange fluxes between air and soil surface were intensively measured at four sampling sites in Guiyang from 21 May to 16 June 2003. Overall, net emissions were obtained from all sampling sites. Soil mercury concentration and solar radiation are proved to be the two most important parameters to control mercury emissions from soil. Meanwhile, a rain event can enhance mercury emission rate significantly. A simple model based on the linear correlation between mercury flux and solar radiation was applied to scale up mercury emissions from soil zones with different mercury concentration ranges. It is observed that mercury emission fluxes from soil in Guiyang are one order of magnitude higher than the value used in early models to represent emissions from global mercuriferous belts which is 1.1 ng $m^{-2}$ $h^{-1}$. The annual mercury emission from soil in Guiyang is calculated to be 408 kg, which highlights that natural emissions from soil contribute significantly to the elevated TGM concentrations in the ambient air in Guiyang.

**Citation:** Feng, X., S. Wang, G. Qiu, Y. Hou, and S. Tang (2005), Total gaseous mercury emissions from soil in Guiyang, Guizhou, China, *J. Geophys. Res.*, *110*, D14306, doi:10.1029/2004JD005643.

## 1. Introduction

[2] Both natural processes and human activities emit a great amount of gaseous mercury (Hg) to the atmosphere [*Lindqvist et al.*, 1991; *Schroeder and Munthe*, 1998]. A recent modeling study [*Lamborg et al.*, 2002] demonstrated that current global anthropogenic Hg emission flux is 2600 t $yr^{-1}$, and that natural emissions reach 1800 t $yr^{-1}$. Certainly, current estimation of natural Hg emissions includes reemission of Hg that originally released by or discharged from both natural and anthropogenic sources [*Schroeder and Munthe*, 1998]. Concentrations of total gaseous Hg (TGM) in the air at remote continental and mid-oceanic locations in both hemispheres have been well documented [*Lindqvist et al.*, 1991; *Fitzgerald et al.*, 1991; *Mason et al.*, 1992; *Slemr et al.*, 1995; *Slemr and Scheel*, 1998; *Schroeder et al.*, 1998; *Ebinghaus et al.*, 2002a, 2002b; *Lindberg et al.*, 2002a; *Lamborg et al.*, 1999; *Lee et al.*, 1998; *Poissant*, 2000]. A small but definite interhemispheric gradient in TGM that reflects global transport from Northern Hemispheric sources is observed [*Ames et al.*, 1998; *Urba et al.*, 1995; *Lamborg et al.*, 2002; *Ebinghaus et al.*, 2002a, 2002b; *Baker et al.*, 2002; *Lindberg et al.*, 2002a; *Schroeder et al.*, 1998; *Temme et al.*, 2003]. The background level of TGM in the Southern Hemisphere is about 1.1 to 1.4 ng $m^{-3}$ [*Ebinghaus et al.*, 2002b; *Baker et al.*, 2002], while that in the Northern Hemisphere is believed to be 1.5 to 2.0 ng $m^{-3}$ [*Ebinghaus et al.*, 2002b; *Schroeder et al.*, 2001; *Lamborg et al.*, 2002]. However, TGM concentrations in urban air are much elevated because of anthropogenic Hg emissions.

[3] TGM concentrations in ambient air in Guiyang, China, were extensively monitored [*Feng et al.*, 2002, 2003, 2004a], and the yearly average TGM concentrations reached 8.4 ng $m^{-3}$ [*Feng et al.*, 2004a]. The elevation of TGM concentration was believed to be mainly derived from anthropogenic Hg emissions, and the main anthropogenic Hg emission source is believed to be from coal combustion for both industry utilization and domestic heating [*Feng et al.*, 2004a]. Hg emission from natural sources, especially from soil was not considered to be important [*Feng et al.*, 2004a]. However, Guiyang is located in the Circum-Pacific Global Mercuriferous Belt, and Hg concentrations in soil in this area are much elevated compared to national background Hg concentration in soil that is 38 ng/g. It is shown that about 63% of total land area has Hg concentrations in soil varying between100 to 200 ng/g, 28% has Hg concentrations varying from 200 to 400 ng/g, 4.8% has Hg


0148-0227/05/2004JD005643

concentrations more than 400 ng/g, and only about 4.2% has Hg concentrations less than 100 ng/g [*Hou*, 2004]. Given that substrate is considered naturally enriched in Hg when concentrations are >100 ng/g [*Gustin et al.*, 2000], soils in 95.8% of area in Guiyang are considered to be enriched with Hg. Numerous studies have showed that Hg enriched soils are important atmospheric Hg emission sources [*Gustin*, 2003; *Gustin et al.*, 2002; *Zehner and Gustin*, 2002; *Gustin et al.*, 2000; *Engle et al.*, 2001; *Rasmussen et al.*, 1998; *Edwards et al.*, 2002], but so far, no studies has addressed the issue of Hg emission from soil in Guiyang. For the first time we investigated the Hg exchange rate between air and soil in Guiyang to better understand Hg emission sources in the area in this paper.

## 2. Materials

### 2.1. Sampling Sites

[4] Guiyang (26°11′–26°55′N, 106°27′–107°03′E), the capital of Guizhou Province, is located in southwestern China, and has a total land area of 2407 $km^2$. The city is situated on Yunnan-Guizhou Plateau with an average altitude of 1050 m above sea level. Its climate represents a typical subtropical humid monsoon with an average annual temperature of 15°C and a precipitation of 1200 mm. Four sampling sites were chosen to measure TGM exchange flux between air and soil surface as shown in Figure 1. The one located at the Institute of Geochemistry, Chinese Academy of Sciences (IGCAS) represents urban area, and Yanlou (YL), Qingyanbao (QYB) and Ganzhang (GZ) sites represent suburb area. The sampling campaigns were conducted from 21 May to 16 June 2003.

### 2.2. Sampling Techniques

[5] The in situ Hg flux measurement was conducted with a dynamic flux chamber (DFC) of Quartz. It is portable and relatively inexpensive. *Xiao et al.* [1991] and *Schroeder et al.* [1989] first introduced DFC method to measurement Hg exchange flux between air and soil/water surface, and afterward, this method was widely used in Hg flux measurement between air and soil/water surface [e.g., *Poissant and Casimir*, 1998; *Rasmussen et al.*, 1998; *Edwards et al.*, 2002; *Ferrara and Mazzolai*, 1998; *Gustin et al.*, 1999; *Carpi and Lindberg*, 1998; *Feng et al.*, 2002, 2004b]. The design of the chamber used in this study is the same as that of *Rasmussen et al.* [1998]. The semicylinder, open-bottom chamber (Ø20 × 60 cm) is placed on soil surface, and is completely exposed to ambient conditions. Three inlet holes with 8mm diameter are applied to the chamber and the inlet holes of the chamber are exposed to ambient wind. Hg flux from the soil surface exposed in the chamber was calculated using equation (1) [*Poissant and Casimir*, 1998; *Xiao et al.*, 1991]:

$$F = (C_o - C_i) \times Q/A \quad (1)$$

where F is the flux of gaseous Hg, which consists of mostly $Hg^0$ [*Schroeder and Munthe*, 1998] in ng Hg $m^{-2}$ $h^{-1}$; $C_o$ and $C_i$ are concentrations of Hg in air of the outlet and inlet of the chamber in ng $m^{-3}$, respectively, and the inlet air is sampled 10 cm above the ground; A is the bottom surface area of the chamber in $m^2$ (0.12 $m^2$); and Q is the flushing flow rate through the chamber in $m^3$ $h^{-1}$ (0.9 $m^3$ $h^{-1}$), and the turnover time of the flux chamber is 37.8 seconds. Hg concentrations were measured twice in the ambient air entering the inlet of the chamber and twice in the air exiting through outlet of the chamber using the two parallel gold traps (A and B) of Tekran 2537A, with a 5 min sampling time at a flow rate of 1.5 L $min^{-1}$. Switching from the inlet

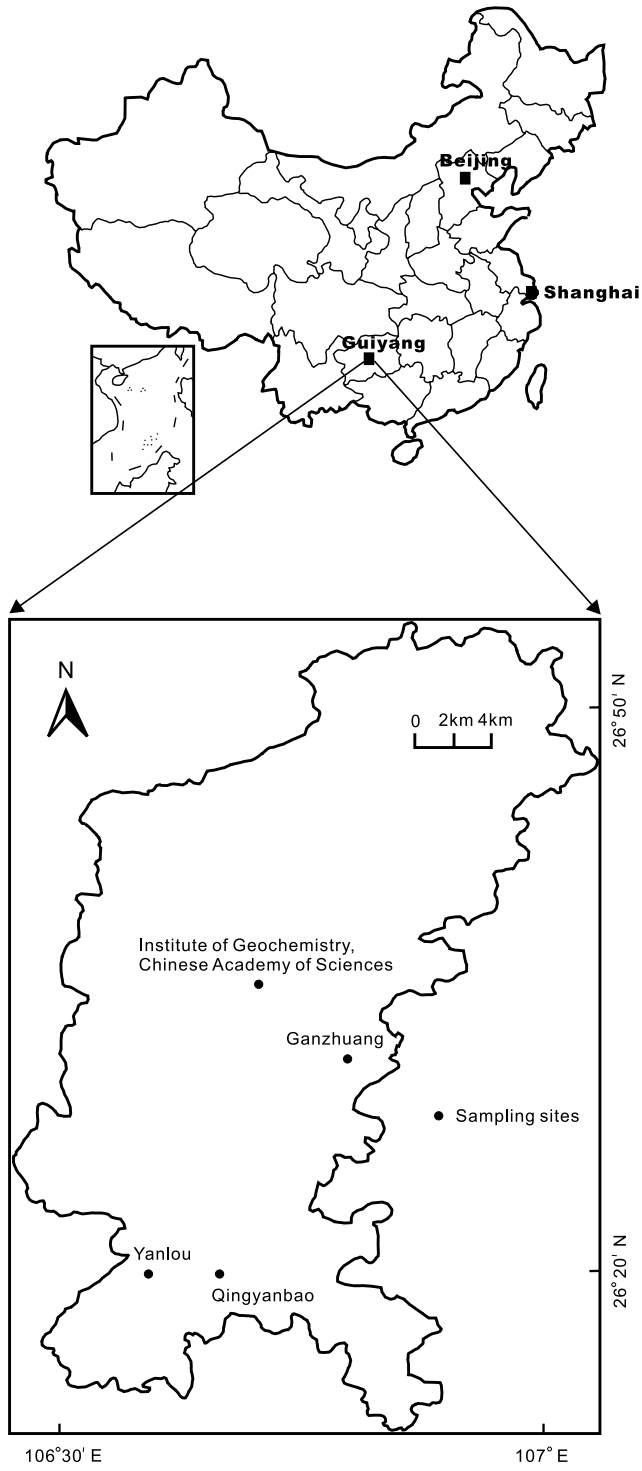


**Figure 1.** The locations of mercury flux measurement sites in Guiyang (solid circles).

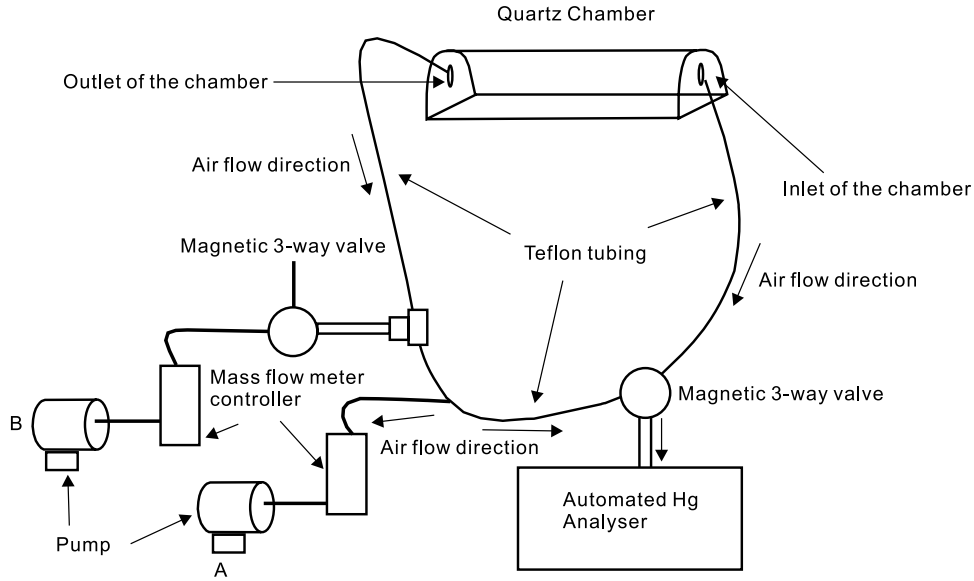


**Figure 2.** The setup of the dynamic flux chamber for measuring Hg flux over soil surface. The automated Hg analyzer used in this study is Tekran 2537A, and its sampling flow rate is 1.5 L $min^{-1}$. The sampling flow rate of pumps A and B that controlled by mass flowmeters is 13.5 and 1.5 L $min^{-1}$, respectively.

and the outlet of the chamber every 10 min was achieved using a magnetic vale provided from Tekran (Tekran 1110) (Figure 2). To keep flow rate through the chamber constant, another mass flow controller combined with the second magnetic valve that is synchronous with the first one was employed to compensate flow rate decrease when Tekran 2537A is sampling air from the inlet of the chamber. Studies [*Zhang et al.*, 2002; *Lindberg et al.*, 2002b; *Gillis and Miller*, 2000] demonstrated that soil Hg emission fluxes measured by DFC operations strongly depend on the flushing air flow rates used, and high flushing flow rates (e.g., $\sim$15–40 L $min^{-1}$ for DFCs of common design) are adopted. It is also shown that high flushing rates can also lead to erroneous flux measurement [*Gillis and Miller*, 2000]. Therefore we used a high flushing flow rate of 15 L $min^{-1}$ (0.9 $m^{-3}$ $h^{-1}$) to prevent the possibility of underestimating Hg flux at low flushing flow rates. The Hg analyzers were calibrated by injecting a volume of Hg saturated air with known concentration [*Feng et al.*, 2004a, 2004b]. The blank of the chamber after being cleaned with diluted $HNO_3$ following with Milli-Q water was measured by sealing the chamber bottom with a Quartz glass plate and the results showed that negligible blanks were detected (0.1–0.2 ng $m^{-2}$ $h^{-1}$).

[6] Representative surface soil sample was collected at each sampling site. The main soil type in the study area is Ultisol. All soil samples were air-dried, milled, and sieved (<80 mesh). The 300–500 mg sample was oxidized with 5 mL concentrated $HNO_3$ + HCl (1:3 v/v) in an Teflon vial using a microwave oven (MDS2000, from CEM, USA) for 50 min. The digested solution then was transferred to a 100 mL volumetric flask, and the volume was made up to 100 ml by adding Mill-Q water. Total Hg concentration was determined using BrCl oxidation and $SnCl_2$ reduction coupled with cold-vapor atomic absorption spectrometry (CVAAS) [*Feng and Hong*, 1999; *Feng et al.*, 2004c]. A standard soil sample GBW-07405 (GSS-5) was used to accomplish QA/QC, and the average total Hg concentration of the geological standard of GBW07405 was $300 \pm 10$ ng $g^{-1}$ (n = 8), which is comparable with certified value of $290 \pm 40$ ng $g^{-1}$. The precision of our method obtained from replicate analysis is less than 5%. The results demonstrated that the pretreatment procedures can quantitatively recover Hg from the soil samples.

[7] The meteorological parameters, such as air temperature, surface soil temperature, wind speed, solar irradiation and relative humidity were monitored using a portable weather station (Global Water IIIB, USA) with a time resolution of 5 min which matched to the 5 min sampling times of the Tekran. The detailed description on the weather station is given by *Feng et al.* [2003, 2004a]. The weather station was located nearby each Hg flux measurement site.

## 3. Results and Discussion

### 3.1. Mercury in Soil of Sampling Sites

[8] Total Hg concentrations in soil at GZ, YL, QYB and IGCAS sites are 150, 220, 250, and 630 ng/g, respectively. Figure 3 depicts total Hg distribution in surface soil of Guiyang [*Hou*, 2004]. We can clearly see that total Hg concentrations obtained from this study are comparable to those displayed in Figure 3. It is also demonstrated that the sampling sites chosen from this study well represent different range of Hg concentrations in soil in Guiyang.

### 3.2. TGM and Mercury Flux Over Soil Surfaces

[9] The Hg fluxes measured over soil surface with dynamic flux chamber as well as the TGM concentrations at 10 cm above the ground at all sampling sites are given in Table 1. The average TGM concentrations at YL, QYB, GZ and IGCAS sites were 8.36, 8.67, 6.18, and 7.84 ng $m^{-3}$, respectively, throughout the flux measurement campaigns. It is obvious that TGM concentrations obtained from these sampling sites are significantly elevated compared

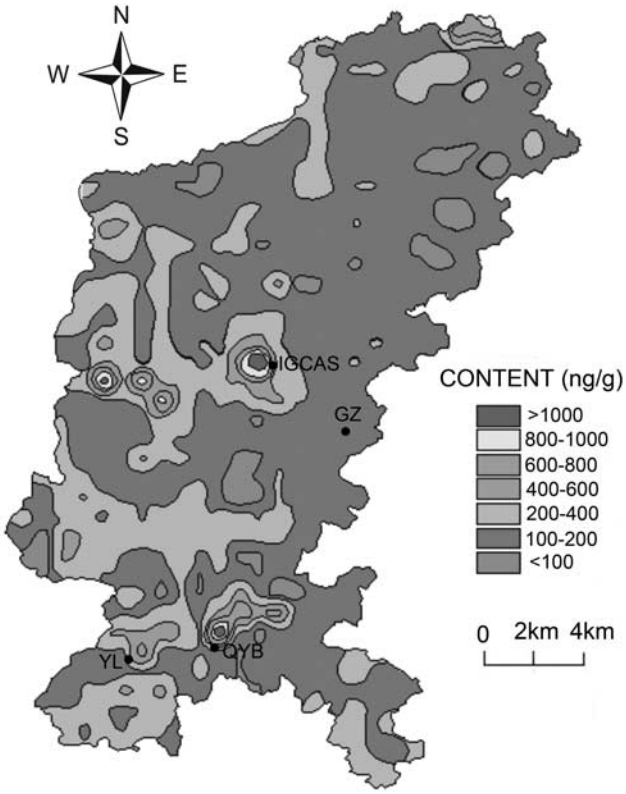


**Figure 3.** Mercury distribution in surficial soil in Guiyang [after *Hou*, 2004]. See color version of this figure at back of this issue.

to the global background value that is believed to be around 1.5 ng $m^{-3}$ [*Lamborg et al.*, 2002]. However, TGM concentrations at these sites are comparable to the reported mean TGM in Guiyang in summer season that is 7.16 ng $m^{-3}$ [*Feng et al.*, 2004a]. High temporal resolved TGM measurement results at four 4 sampling sites are depicted in Figure 4. It is generally observed that TGM concentration peaked during daytime when strong Hg emission fluxes appeared as discussed in the following section. The correlations between mercury fluxes and TGM concentrations at 4 sampling sites were investigated as shown in Figure 5. It is observed that TGM concentrations correlated significantly ($p < 0.01$) with mercury flux at YL and QYB sites, which are relatively far away from anthropogenic sources such as coal fired power plant. Weak correlations between TGM concentrations and mercury fluxes were also obtained at GZ and IGCAS sites (Figure 5), which are situated in and close to downtown, respectively. This observation highlights that apart from anthropogenic Hg emission sources [*Feng et al.*, 2004a], Hg emission from soil in Guiyang may contribute significantly to the distribution of TGM in ambient air.

[10] The Hg flux results as displayed in Table 1 have been corrected with the field blanks. Both evasion from soil and deposition to soil were recorded at 4 sampling sites. Overall, net emissions were however obtained from all sampling sites, and the average net emission fluxes at YL, QYB, GZ and IGCAS are 44.4, 15.0, 0.4, and 31.8 ng $m^{-2}$ $h^{-1}$, respectively. Except for GZ site where Hg concentration in soil is the lowest, measured Hg emission fluxes at the three Hg enriched sites are significantly higher than the average Hg emission flux measured at a background site in Canada during summer season that is 2.95 ng $m^{-2}$ $h^{-1}$ [*Poissant and Casimir*, 1998]. This observation also supports the hypothesis that Hg emissions from soil in Guiyang may contribute significantly to the distribution of TGM in ambient air.

[11] A clear diurnal pattern of Hg flux is obtained from all sampling sites as shown in Figure 6 with Hg evasion during the daytime reaching a maximum at midday followed by reduced fluxes which became deposition during the nighttime period. Many studies [e.g., *Poissant et al.*, 1999] demonstrated dry deposition of mercury to soil surface occurred especially during night period using dynamic flux chamber method to measure flux, which highlights that soil surface can adsorb mercury vapor when TGM concentrations in soil air are lower than that in ambient air. Meanwhile the Hg fluxes mimicked the solar irradiation (Figure 7), and the correlation coefficients between the two parameters are 0.86 ($n = 139$, $p < 0.01$) at YL, 0.74 ($n = 142$, $p < 0.01$) at QYB, 0.74 ($n = 135$, $p < 0.01$) at GZ, and 0.71 ($n = 737$, $p < 0.01$) at IGCAS, respectively. Hg flux is positively correlated with air temperature (Figure 8), and negatively correlated with relative humidity (Figure 9) at all sampling sites. These observations agree well with previous studies [e.g., *Poissant and Casimir*, 1998; *Engle and Gustin*, 2002].

[12] Many laboratory and field studies demonstrated that Hg concentration in soil is the key factors controlling Hg emission rate from soil to the air [e.g., *Bahlmann et al.*,

**Table 1.** Statistical Summary of the Parameters Measured Over the Soil Surface[a]

| Sampling Site | Parameter | Average | Median | SD | Coefficient of Variation, % | Minimum | Maximum | N |
|---|---|---|---|---|---|---|---|---|
| YL | TGM (ng $m^{-3}$) | 8.36 | 7.66 | 2.60 | 31.1 | 4.68 | 18.4 | 277 |
| YL | evasion | 52.2 | 16.1 | 64.2 | 123.1 | 0.1 | 250.6 | 122 |
| YL | deposition | 11.2 | 9.1 | 7.9 | 70.3 | 0.9 | 25.7 | 17 |
| QYB | TGM (ng $m^{-3}$) | 8.67 | 7.99 | 2.59 | 29.9 | 5.2 | 20.1 | 283 |
| QYB | evasion | 29.9 | 10.5 | 42.4 | 142.2 | 0.02 | 199.3 | 90 |
| QYB | deposition | 10.7 | 7.9 | 10.1 | 94.9 | 0.06 | 45.6 | 52 |
| GZ | TGM (ng $m^{-3}$) | 6.18 | 5.9 | 1.94 | 31.4 | 3.1 | 16.3 | 264 |
| GZ | evasion | 22.3 | 20.8 | 15.0 | 67.4 | 1.1 | 55.3 | 46 |
| GZ | deposition | 11.0 | 9.6 | 6.9 | 63.2 | 0.1 | 39.7 | 89 |
| IGCAS | TGM (ng $m^{-3}$) | 7.84 | 6.90 | 3.89 | 49.6 | 1.8 | 45.2 | 1480 |
| IGCAS | evasion | 34.4 | 27.5 | 27.09 | 78.6 | 0.5 | 236.4 | 698 |
| IGCAS | deposition | 15.0 | 9.7 | 15.49 | 102.8 | 0.4 | 59.4 | 39 |

[a]Fluxes are expressed in ng $m^{-2}$ $h^{-1}$.

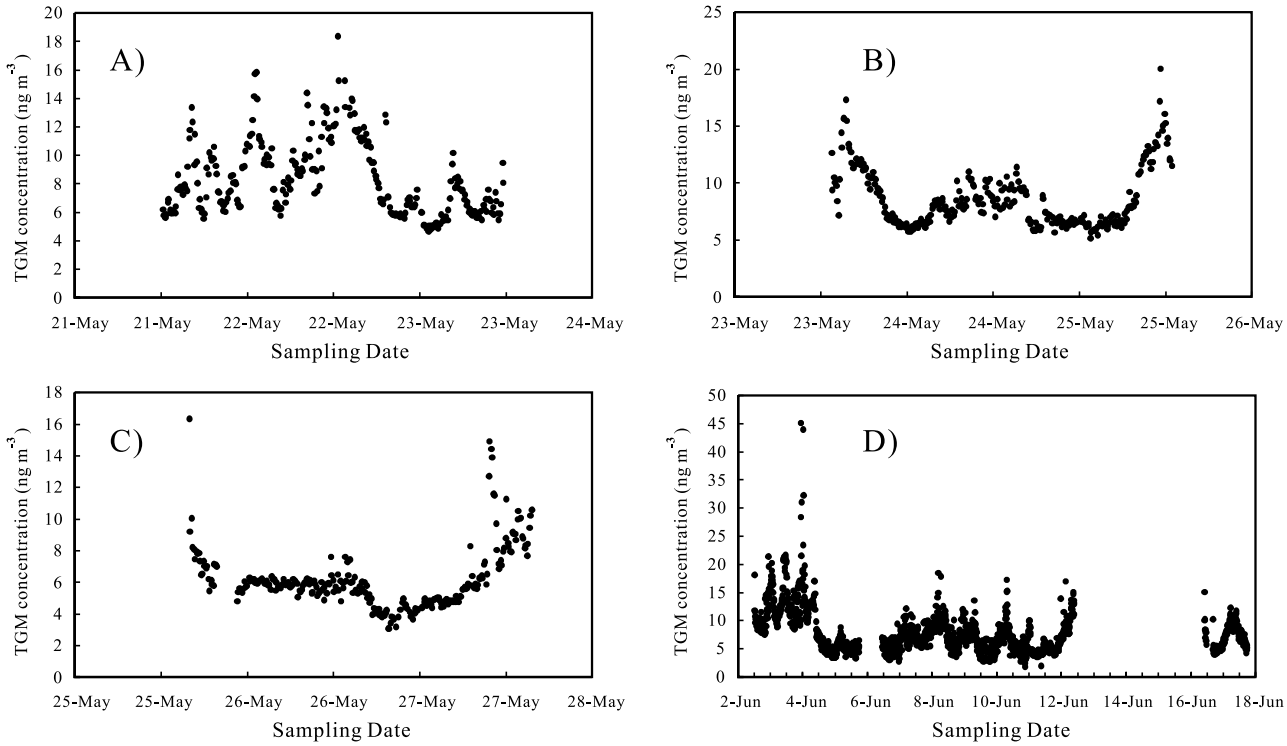


**Figure 4.** TGM concentrations in the air 10 cm above the soil surface during all flux measurement campaigns (a) at Yanlou (YL) site, (b) at Qingyanbao (QYB) site, (c) at Ganzhuang (GZ) site, and (d) at Institute of Geochemistry, Chinese Academy of Sciences (IGCAS) site.

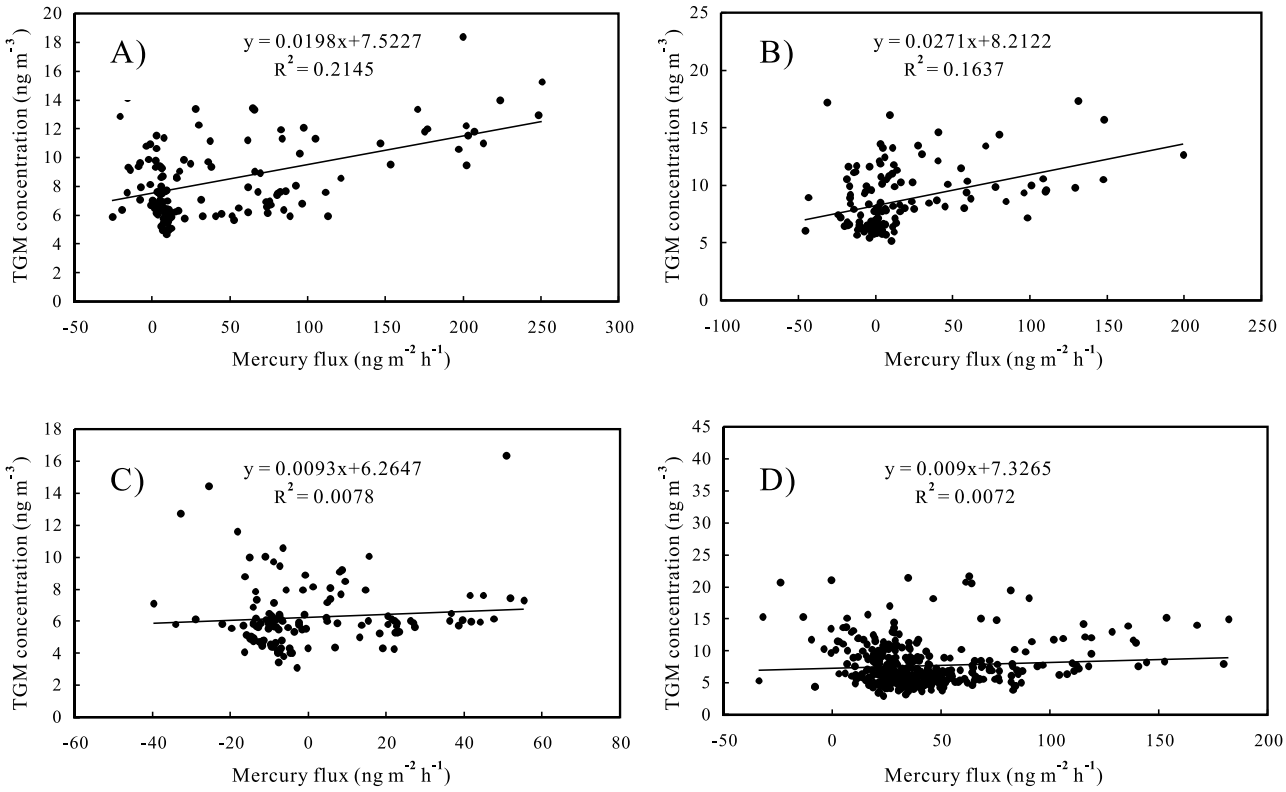


**Figure 5.** The correlations between TGM concentrations in the air and Hg flux at four sampling sites: (a) at Yanlou (YL) site, (b) at Qingyanbao (QYB) site, (c) at Ganzhuang (GZ) site, and (d) at Institute of Geochemistry, Chinese Academy of Sciences (IGCAS) site.

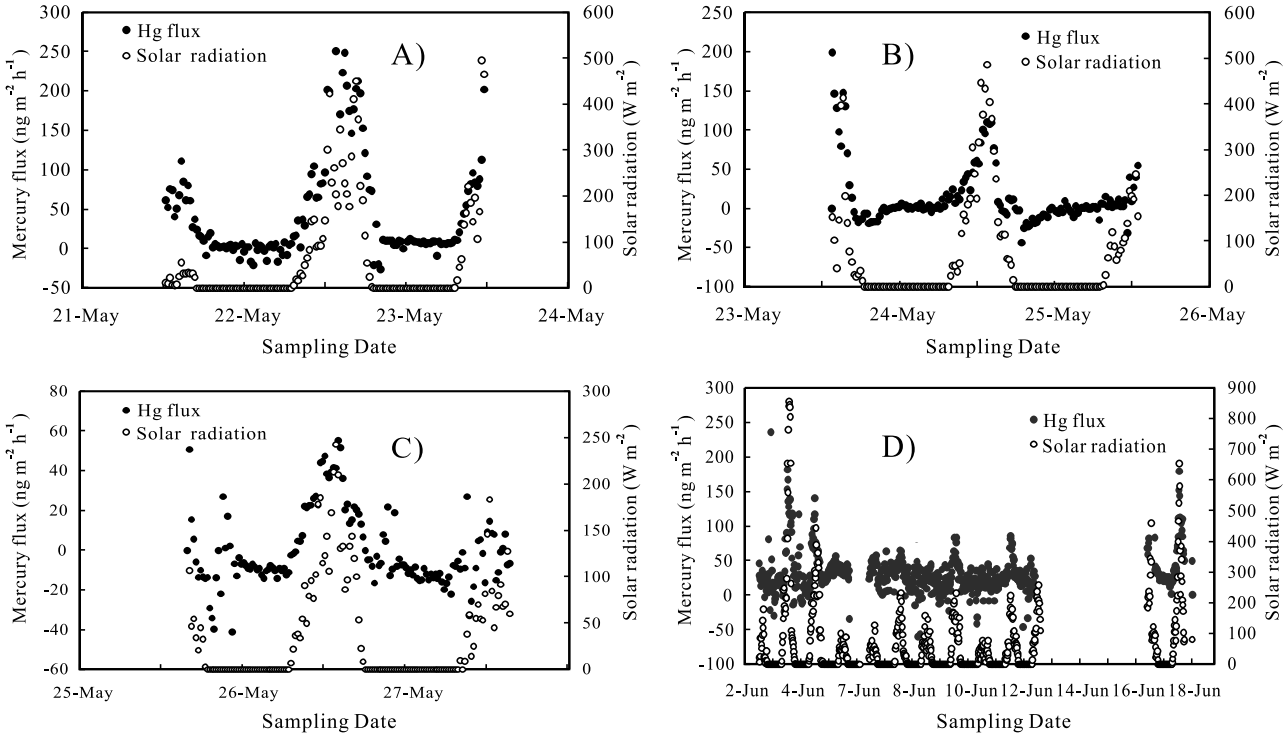


**Figure 6.** Relationships between Hg flux and solar radiation at four sampling sites: (a) at Yanlou (YL) site, (b) at Qingyanbao (QYB) site, (c) at Ganzhuang (GZ) site, and (d) at Institute of Geochemistry, Chinese Academy of Sciences (IGCAS) site.

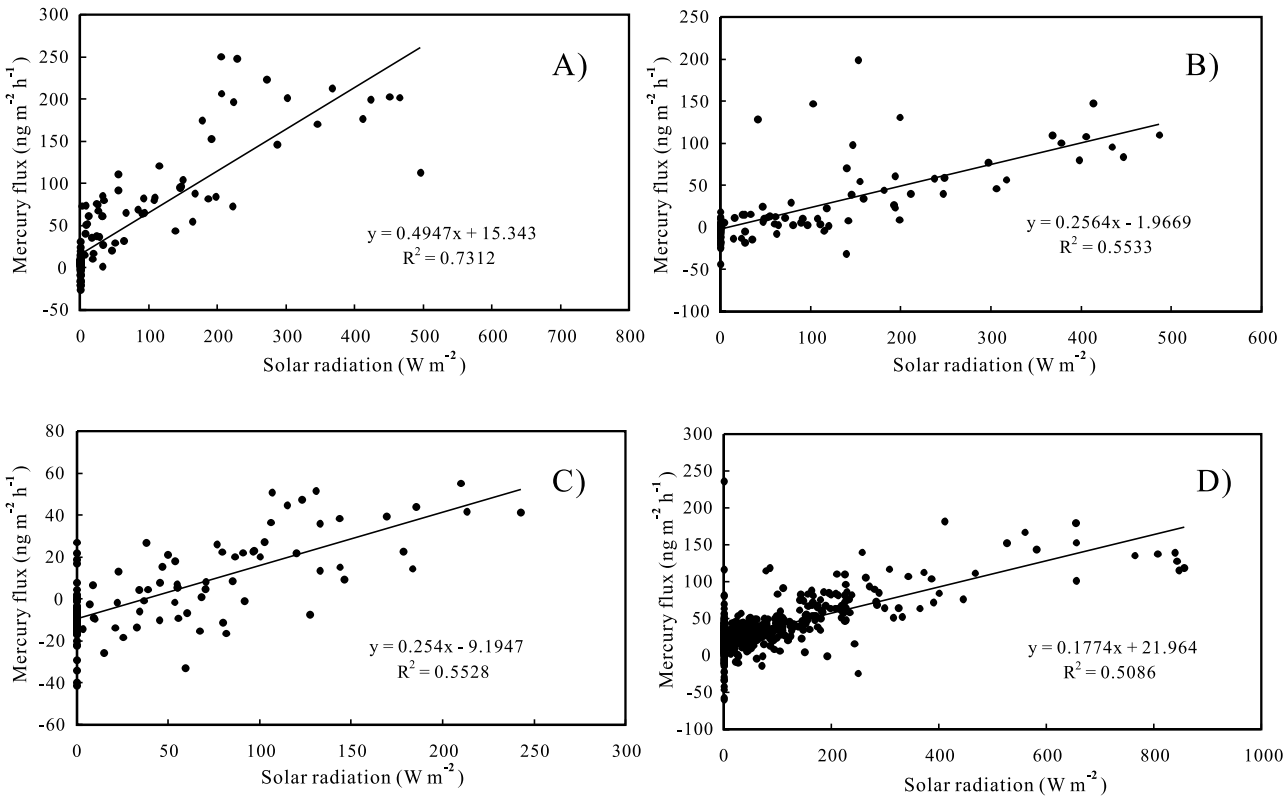


**Figure 7.** The correlations between Hg flux and solar radiation at four sampling sites: (a) at Yanlou (YL) site, (b) at Qingyanbao (QYB) site, (c) at Ganzhuang (GZ) site, and (d) at Institute of Geochemistry, Chinese Academy of Sciences (IGCAS) site.

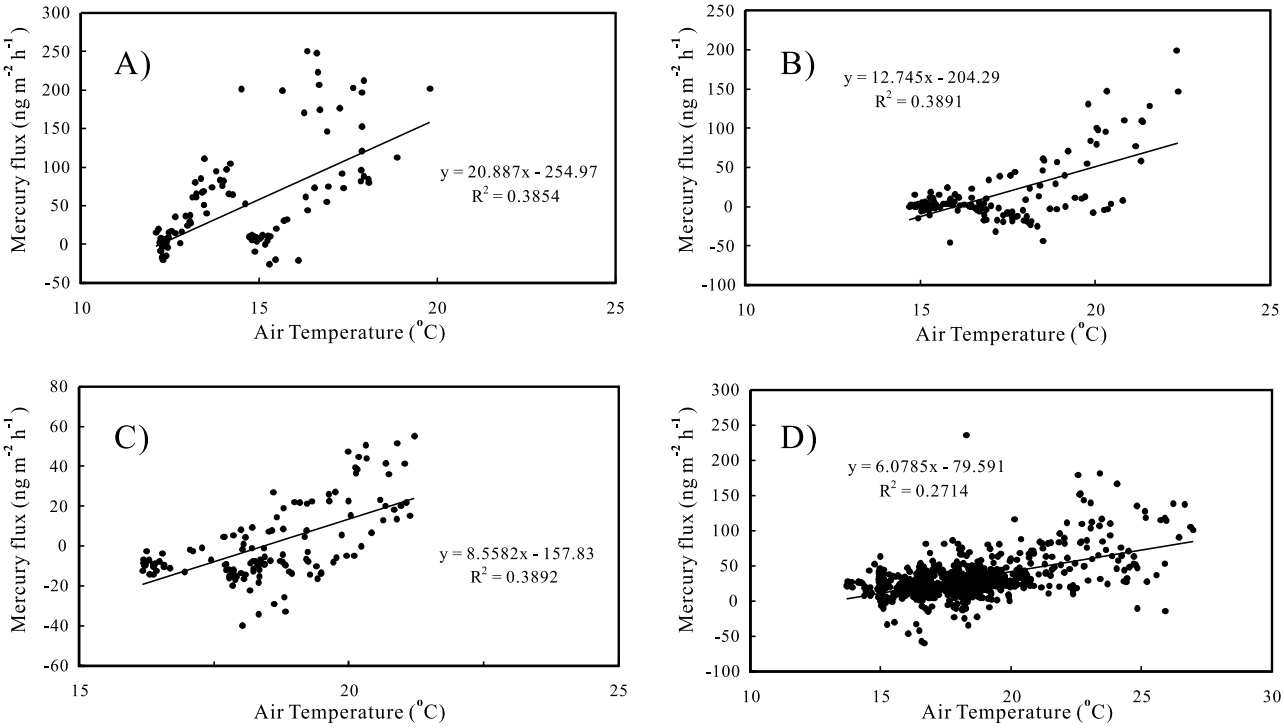


**Figure 8.** Correlation between Hg flux and air temperature at all sampling sites: (a) at Yanlou (YL) site, (b) at Qingyanbao (QYB) site, (c) at Ganzhuang (GZ) site, and (d) at Institute of Geochemistry, Chinese Academy of Sciences (IGCAS) site.

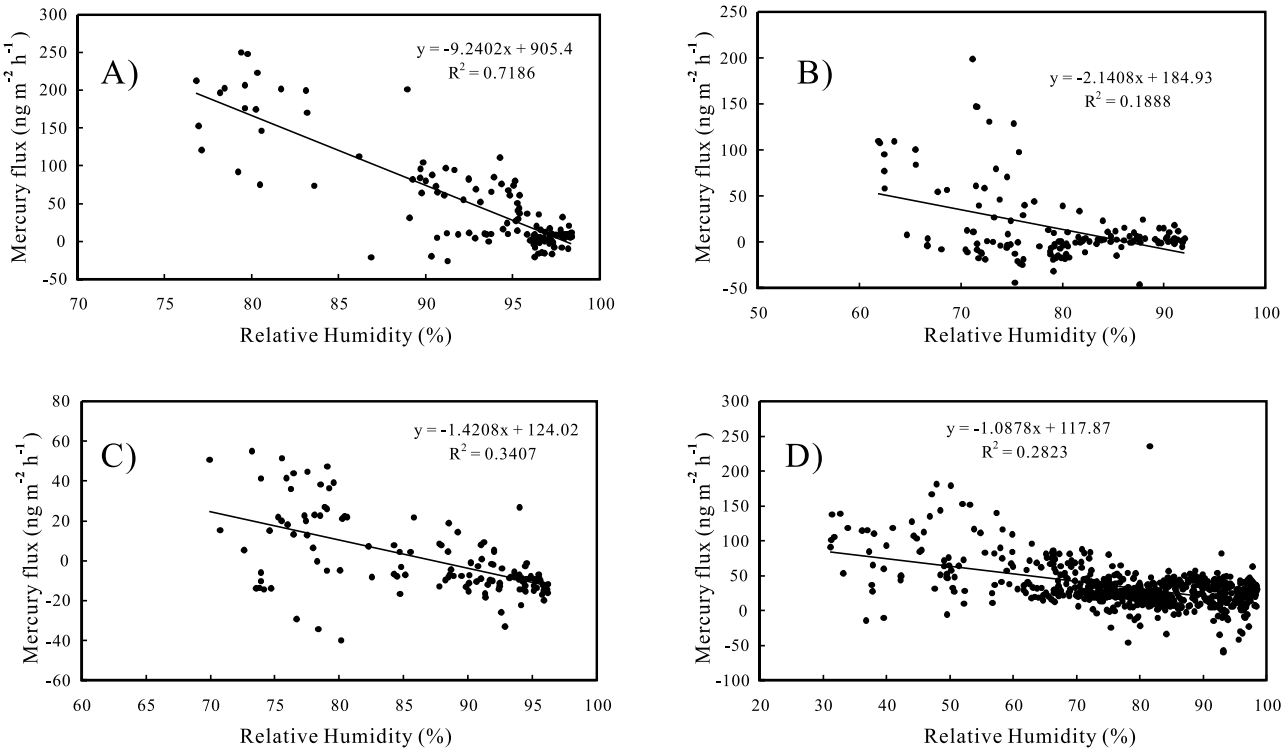


**Figure 9.** Correlation between Hg flux and relative humidity at all sampling sites: (a) at Yanlou (YL) site, (b) at Qingyanbao (QYB) site, (c) at Ganzhuang (GZ) site, and (d) at Institute of Geochemistry, Chinese Academy of Sciences (IGCAS) site.

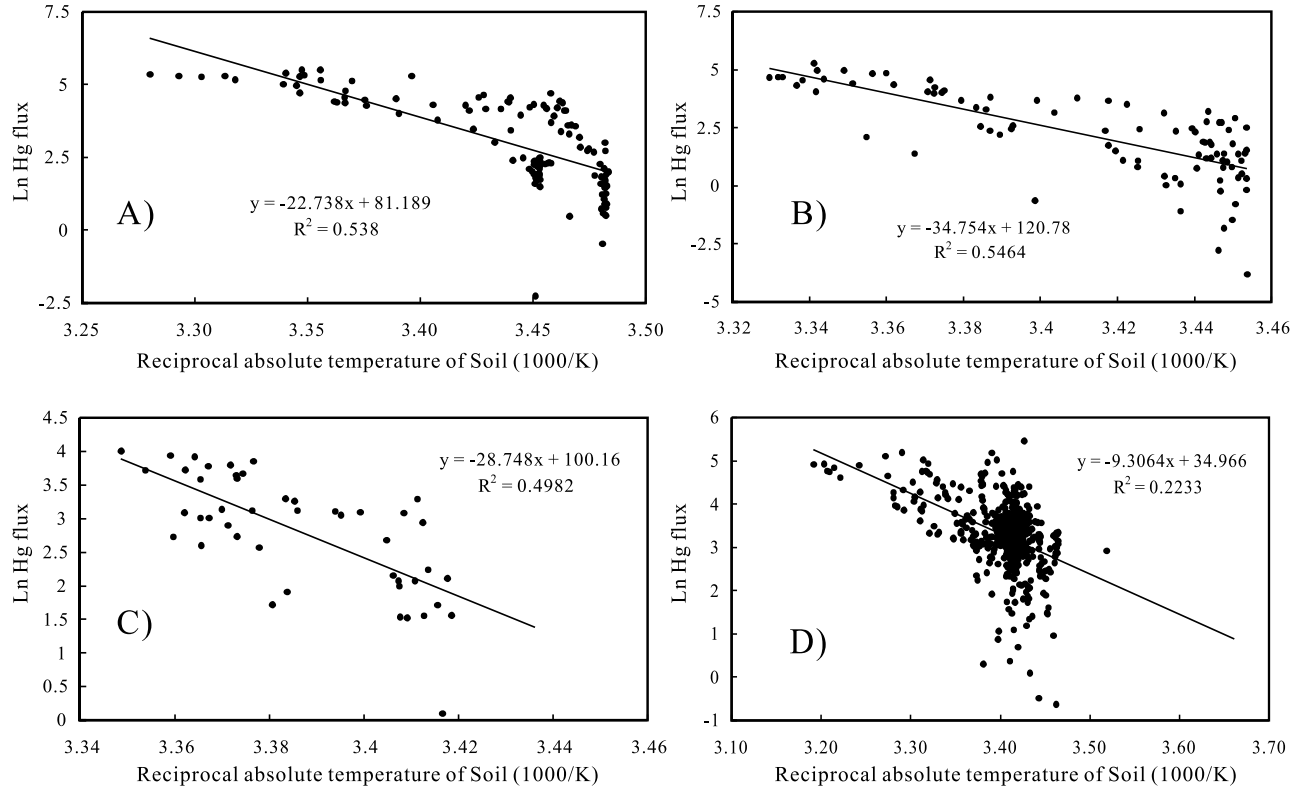


**Figure 10.** The Arrhenius relationships between Hg flux and soil temperature at all sampling sites: (a) at Yanlou (YL) site, (b) at Qingyanbao (QYB) site, (c) at Ganzhuang (GZ) site, and (d) at Institute of Geochemistry, Chinese Academy of Sciences (IGCAS) site.

2004a; *Zehner and Gustin*, 2002; *Feng et al.*, 1996; *Schluter*, 2000]. Total Hg concentration in soil at YL site is almost equivalent to that at QYB as stated in section 3.1. However, we observed much stronger Hg emission fluxes at YL than those at QYB even at similar meteorological conditions as shown in Figure 6a and 6b. A mild rain event occurred early afternoon on 21 May 2003 when flux measurement campaign initiated as we can see from the low intensities of solar radiation during that period of time in Figure 6a. The rain event which lasted out for a few hours definitely increased the moisture of soil (unfortunately the moisture of soil was not monitored during the measurements campaigns). The effect of soil moisture on Hg emission fluxes from soils was first noted during an international field campaign in Reno, Nevada, where a tremendous increase of Hg emission flux one hour after the rain event was observed [*Lindberg et al.*, 1999]. Laboratory studies also demonstrated soil moisture has an overall strong effect to promote the emission of Hg from soils at certain conditions [*Bahlmann et al.*, 2004b]. Therefore the discrepancy of Hg emission fluxes obtained at these two sites is attributed to the soil moisture difference.

[13] The temperature dependence of Hg fluxes over the soil surface is clearly shown by using Arrhenius equation (equation (2)),

$$k = Ae^{-Ea/RT} \quad (2)$$

where k is Hg flux, R is the gas constant (1.9872 cal $k^{-1}$ $mol^{-1}$), T is soil temperature in degrees Kelvin, A is the preexponential factor and Ea is the activation energy. As shown in Figure 10, a significant correlation between Hg emission flux and soil temperature depicted by Arrhenius equation is observed at all sampling sites. The apparent activation energies for TGM emission at YL, QYB, GZ and IGCAS are 45.2, 69.1, 57.1 and 18.6 kcal $mol^{-1}$, respectively. The Ea obtained from IGCAS sampling site agrees well with other published soil Hg activation energies (17.3–25.8 kcal $mol^{-1}$) [*Carpi and Lindberg*, 1998; *Poissant and Casimir*, 1998; *Kim et al.*, 1995; *Lindberg et al.*, 1995]. However, the apparent activation energies observed from the other 3 sampling sites are much elevated compared to published literature values. This discrepancy may be derived from the soil characteristics and differences of land use among the sites. It is obviously that much work is needed to elucidate the elevation of the apparent activation energies observed from these sites.

[14] The significant correlations between Hg emission flux and soil temperature observed in our study seem to illustrate that soil temperature is an important driving force of Hg emission from soil. *Zhang and Lindberg* [1999] proposed 9 possible scenarios of Hg(II) reduction reactions in soils, which include solution phase reduction in the dark by organic acids or by $H_2O_2$ under basic conditions; direct photolysis of both $Hg(OH)_2$ and Hg (II)-organic acid complexes in soil solution; the light-induced, $O_2$-catalyzed, dissolved organic carbon (DOC) assisted reduction in solution phase; the Fe(III)-organic acid complex-assisted light-induced reduction in solution phase; the light-sensitized DOC-assisted reduction solution phase; surface direct pho-

tolysis complexes of Hg(II) with organic acid ligands or hydroxide ions in solid phase; Fe(III) and organic assisted surface reduction in solid phase; surface catalysis photoinduced reduction by $TiO_2$ and $ZnO_2$; and light-induced free radical mediated reduction of Hg(II) in the presence of humic substances, organic acids, and soluble reactive Fe(III) species. However, recent laboratory studies clearly demonstrated that solar radiation is the more dominant process controlling Hg emissions from naturally enriched substrates than soil temperature [*Gustin et al.*, 2002], and that light induced Hg emission flux is independent of the soil temperature [*Bahlmann et al.*, 2004a]. Photoreduction of divalent Hg species both in soil solution and solid phases at the soil surface is the basic driving force of Hg emission from soil [*Zhang and Lindberg*, 1999; *Gustin et al.*, 2002; *Bahlmann et al.*, 2004a]. Our study also showed that the intensity of solar radiation has the most significant correlation with Hg flux among all meteorological parameters, which in a way supports that light induced Hg emission flux definitely predominates in soil/air Hg exchange at naturally Hg enriched areas. Laboratory studies concerning the correlations between Hg exchange flux over soil and meteorological parameters such as soil temperature [*Gustin et al.*, 1997], air temperature and relative humidity are rare from open literature. Since these meteorological parameters such as air temperature, soil temperature, and relative humidity in some way correlate with the intensity of solar radiation, the significant correlations between Hg flux and these meteorological parameters may be a reflection of the correlation between Hg exchange flux and solar radiation. Definitely more study is needed to address the effects of such meteorological parameters on Hg emission flux over soil to better understand and quantify Hg emission rate from soil.

### 3.3. Quantifying Mercury Emission From Soil in Guiyang

[15] In recent years, many efforts were diverted to scaling of atmospheric Hg emissions from naturally enriched areas [*Gustin*, 2003; *Zehner and Gustin*, 2002; *Engle and Gustin*, 2002; *Engle et al.*, 2001; *Coolbaugh et al.*, 2002]. *Zehner and Gustin* [2002] estimated Hg emission flux from natural substrate in Nevada based upon in situ Hg flux measurements and geographic information systems (GIS) approach. *Engle et al.* [2001] used in situ Hg emission flux measurement, along with data from laboratory studies and statistical analysis to scale up Hg emissions for the naturally enriched Ivanhoe Mining District, Nevada. *Engle and Gustin* [2002] and *Coolbaugh et al.* [2002] estimated annual Hg emission rates from three natural enriched areas in Nevada and California. Though most studies were accomplished in Nevada and California, these scaling results suggest that the value of 1.1 ng $m^{-2}$ $h^{-1}$ used in early models [*Lindqvist et al.*, 1991; *Mason et al.*, 1994] to represent emissions from global mercuriferous belts is too low by at least three times [*Gustin*, 2003].

[16] In order to scale up Hg emission from soil in Guiyang area, Guizhou, China, the most important parameters controlling Hg emission from soil have to be selected. Studies showed that geological parameters, such as substrate Hg concentration, rock type, degree of hydrothermal alteration and the presence of heat sources and geologic structures, dominate in controlling the magnitude of Hg emissions from natural sources [*Gustin*, 2003]. Guiyang is located at a geologically stable area without large faults and current geothermal activities, and the bedrocks are limestone and dolomite. Therefore the most important geological parameter to control the magnitude of Hg emission from soil is the soil Hg concentration. As shown in Figure 3, Hg concentrations in soil from Guiyang area vary from a range from <100 to >1000 ng $g^{-1}$, so that the demonstrated log-log relationship between Hg flux and soil Hg concentration obtained by *Gustin* [2003] is not easily depicted in our case. According to Hg concentrations in soil in Guiyang, we can roughly divide soil from Guiyang into three zones: (1) zone A, soil with Hg concentrations less than 200 ng $g^{-1}$; (2) zone B, soil with Hg concentrations from 200 to 400 ng $g^{-1}$; and (3) zone C, soil with Hg concentration higher than 400 ng $g^{-1}$, which consist of 67%, 28.3% and 4.7% of the total area of Guiyang, respectively. We assume that the in situ Hg flux measurements from different sampling sites represent soil from these three soil zones.

[17] It is known that meteorological parameters especially solar radiation, temperature and precipitation dictate diel trends of Hg emission flux. However, recent studies [e.g., *Gustin*, 2003] and our study all demonstrated that solar radiation is the most important factor to drive the diel pattern of Hg emission flux from soil as state in section 3.2. Equations (3) to (6) (Figure 7) illustrate the linear correlation between Hg flux and the intensity of solar radiation at YL, QYB, GZ and IGCAS, respectively,

$$F1 = 0.4947S + 15.343,\ R^2 = 0.7312 \quad (3)$$

$$F2 = 0.2564S - 1.9669,\ R^2 = 0.5533 \quad (4)$$

$$F3 = 0.254S - 9.1947,\ R^2 = 0.5528 \quad (5)$$

$$F4 = 0.1774S + 21.964,\ R^2 = 0.5086 \quad (6)$$

where F1, F2, F3 and F4 are modeled Hg flux at YL, QYB, GZ and IGCAS, respectively; S is the intensity of solar radiation; R is the correlation coefficient. Using equations (3)–(6), we calculated modeled Hg flux according to the intensity of solar radiation during the sampling campaign and listed the daily average of modeled Hg flux in Table 2. Meanwhile we also computed the daily average of measured Hg flux as showed in Table 2. We can see that in most case the modeled daily average Hg fluxes agree well with the measured fluxes, and that the largest discrepancies (more than 60%) occurred when Hg fluxes were very low. Low Hg fluxes were usually obtained during cloudy weather conditions, when the sun light was not very strong. Therefore other less important parameters such as soil temperature, wind speed [*Gillis and Miller*, 2000] and so on which are not considered in the model may alter mercury flux causing large discrepancies between the measured and modeled Hg fluxes. Therefore we believe

**Table 2.** Comparison of Measured Daily Hg Flux and Modeled Flux[a]

| Sampling Site | Sampling Time | Measured Daily Average Hg Flux | Modeled Daily Average Hg Flux | Coefficient of Variation,[b] % |
|---|---|---|---|---|
| YL | 21 May 1215 to 22 May 1215 | 25.6 | 25.4 | −0.8 |
| YL | 22 May 1130 to 23 May 1130 | 65.3 | 67.0 | 2.6 |
| QYB | 23 May 1330 to 24 May 1330 | 21.1 | 19.8 | −6.1 |
| QYB | 24 May 1250 to 25 May 12:50 | 8.0 | 15.3 | 62.6 |
| GZ | 25 May 1555 to 26 May 15:55 | 4.8 | 2.4 | −65.3 |
| GZ | 26 May 1555 to 27 May 15:55 | −4.6 | −2.2 | −69.8 |
| IGCAS | 2 June 1210 to 3 June 1210 | 25.3 | 30.7 | 19.0 |
| IGCAS | 3 June 1210 to 4 June 1210 | 51.3 | 47.8 | −7.0 |
| IGCAS | 4 June 1210 to 5 June 1210 | 39.0 | 32.9 | −17.0 |
| IGCAS | 6 June 1040 to 7 June 1040 | 32.9 | 25.7 | −24.5 |
| IGCAS | 7 June 1040 to 8 June 1040 | 25.3 | 30.0 | 17.1 |
| IGCAS | 8 June 1040 to 9 June 1040 | 19.5 | 26.4 | 30.2 |
| IGCAS | 9 June 1040 to 10 June 1040 | 25.7 | 28.8 | 11.4 |
| IGCAS | 10 June 1040 to 11 June 1040 | 21.5 | 25.2 | 15.5 |
| IGCAS | 11 June 1040 to 12 June 1040 | 29.0 | 29.9 | 3.1 |
| IGCAS | 16 June 1600 to 17 June 1600 | 44.2 | 39.3 | −11.7 |

[a]Values are in ng $m^{-2}$ $h^{-1}$.
[b]Coefficient of variation = (measured daily Hg flux − modeled daily Hg flux) × 2 × 100/(measured daily Hg flux + modeled daily Hg flux).

that our models could satisfactorily predict Hg emission flux at different sampling sites.

[18] Equations (5) and (6) are used to predict Hg emission flux at zone A, and C, respectively. For zone B, however, two different equations were obtained. As discussed in section 3.2, rain effect clearly enhanced Hg emission flux due to increase of soil moisture at YL sampling site. In order to eliminate the bias (over estimate) from rain effect, we select equation (4) to predict Hg flux from soil in zone B. We applied the high temporal resolved solar radiation data (every 5 min) collected in a previous study from November 2001 to November 2002 in Guiyang [*Feng et al.*, 2004a] to equations (4)–(6), calculated the annual average Hg emission rates from 3 zones and depicted in Table 3. It is obvious that Hg emission fluxes from soil in Guiyang are one order of magnitude higher than the value used in early models to represent emissions from global mercuriferous belts which is 1.1 ng $m^{-2}$ $h^{-1}$ [*Lindqvist et al.*, 1991].

[19] The annual Hg emission from soil in Guiyang is calculated to be 408 kg. A recent study [*Tang*, 2004] showed that coal combustion which is believed to be the largest anthropogenic Hg emission source in the region contributed about 639 kg gaseous Hg (gaseous divalent Hg and elemental Hg) to the ambient air in 2002. Hg emission from coal combustion is projected to increase annually due to the demand from continuing economic growth in Guiyang. Although human activities may emit more mercury to the ambient air compared to natural sources, our preliminary data highlight that natural emissions from soil contribute significantly as well to the elevated TGM concentrations in the ambient air in Guiyang.

[20] Of course, there are uncertainties on our estimation of mercury emission from soil in Guiyang because many simplifications were applied. First of all, the effects of other meteorological parameters such as soil and air temperature to Hg flux were not considered, though they may play minor role. Secondly, rain effect which could significantly increase mercury emissions from soil for a certain period of time after rain was not considered in our simple model. Finally, the effect of vegetation cover on mercury flux from soil was not considered at all in our models. It is obvious that more work is needed to more precisely estimate mercury emission from soil in Guiyang.

## 4. Conclusions

[21] Guiyang is located in the Circum-Pacific Global Mercuriferous Belt, and Hg concentrations in soil in this area are much elevated compared to national background Hg concentration in soil. A clear diurnal pattern of Hg flux between air and soil is obtained with Hg evasion during the daytime reaching a maximum at midday followed by reduced fluxes which became deposition during the nighttime period. The diel pattern of Hg flux is mainly driven by solar radiation.

[22] Soil Hg concentrations and solar radiation were used to scale up Hg emission from soil in Guiyang. It is observed that Hg emission fluxes from soil in Guiyang are one order of magnitude higher than the value used in early models to represent emissions from global mercuriferous belts which is 1.1 ng $m^{-2}$ $h^{-1}$. The annual Hg emission from soil in Guiyang is calculated to be 408 kg, while the coal combustion which is believed to be the largest anthropogenic Hg emission source in the region contributed about 639 kg $yr^{-1}$ gaseous Hg (gaseous divalent Hg and elemental Hg) to the ambient air. Our preliminary data highlight that natural emissions from soil

**Table 3.** Modeled Mercury Emission Fluxes From Different Soil Zones in Guiyang[a]

| | Zone A | Zone B | Zone C |
|---|---|---|---|
| Mercury concentration range, ng $g^{-1}$ | <200 | 200–400 | >400 |
| Total land area, $km^2$ | 1612 | 680 | 114 |
| Area average flux, ng $m^{-2}$ $h^{-1}$ | 16.5 | 23.2 | 37.0 |
| Annual flux, kg $yr^{-1}$ | 138.2 | 232.3 | 37.0 |

[a]Total mercury emission from soil in Guiyang is 407.5 kg $yr^{-1}$.

contribute significantly to the elevated TGM concentrations in the ambient air in Guiyang.

[23] **Acknowledgment.** This research was financially supported by Chinese Academy of Sciences through Innovation Project (KZCX3-SW-443) and by the Chinese Natural Science Foundation (40173037, 40203009, and 40273041).

## References

Ames, M., G. Gullu, and I. Olmez (1998), Atmospheric mercury in the vapor phase, and in fine and coarse particulate matter at Perch River, New York, *Atmos. Environ.*, *32*, 865–872.

Bahlmann, E., R. Ebinghaus, and W. Ruck (2004a), Influence of solar radiation on mercury emission fluxes from soils, *Mater. Geoenviron.*, *51*, 787–790.

Bahlmann, E., R. Ebinghaus, and W. Ruck (2004b), The effect of soil moisture on the emission of mercury from soils, *Mater. Geoenviron.*, *51*, 791–794.

Baker, P. G. L., E.-G. Brunke, F. Slemr, and A. M. Crouch (2002), Atmospheric mercury measurements at Cape Point, South Africa, *Atmos. Environ.*, *36*, 2459–2465.

Carpi, A., and S. E. Lindberg (1998), The sunlight mediated emission of elemental mercury from soil amended with municipal sewage sludge, *Environ. Sci. Technol.*, *31*, 2085–2091.

Coolbaugh, M. F., M. S. Gustin, and J. J. Yytuba (2002), Annual emissions on mercury to the atmosphere from three natural source areas in Nevada and California, *Environ. Geol.*, *42*, 338–349.

Ebinghaus, R., H. H. Kock, A. M. Coggins, T. G. Spain, S. G. Jennings, and C. Temme (2002a), Long-term measurements of atmospheric mercury at Mace Head, Irish west coast, between 1995 and 2001, *Atmos. Environ.*, *36*, 5267–5276.

Ebinghaus, R., H. H. Kock, C. Temme, J. W. Einax, A. G. Lowe, A. Richter, J. P. Burrows, and W. H. Schroeder (2002b), Antarctic springtime depletion of atmospheric mercury, *Environ. Sci. Technol.*, *36*, 1238–1244.

Edwards, G. C., P. E. Rasmussen, W. H. Schroeder, K. J. Kemp, G. Dias, L. Halfpenny-Mitchell, D. Wallace, and A. Steffen (2002), Measurements of mercury fluxes from natural sources, paper presented at 2002 Canadian MITE-RN Annual Symposium, Can. Geol. Surv., Ottawa.

Engle, M. A., and M. S. Gustin (2002), Scaling up atmospheric mercury emissions from three naturally enriched areas: Flowery Peak, Nevada, Peavine Peak, Nevada and Long Valley Caldera, California, *Sci. Total Environ.*, *290*, 91–104.

Engle, M. A., M. S. Gustin, and H. Zhang (2001), Quantifying natural source mercury emissions from the Ivanhoe mining district, North-central Nevada, USA, *Atmos. Environ.*, *35*, 3987–3997.

Feng, X., and Y. Hong (1999), Modes of occurrence of mercury in coals from Guizhou, People's Republic of China, *Fuel*, *78*, 1181–1188.

Feng, X., Y. Chen, and W. Zhu (1996), Vertical fluxes of volatile mercury over soil surfaces (in Chinese), *Environ. Sci.*, *17*(2), 20–22.

Feng, X., J. Sommar, O. Lindqvist, and Y. Hong (2002), Occurrence, emission and deposition of mercury from coal combustion in the Province Guizhou, China, *Water Air Soil Pollut.*, *139*, 311–324.

Feng, X., S. Tang, L. Shang, H. Yan, J. Sommar, and O. Lindqvist (2003), Total gaseous mercury in the air of Guiyang, PR China, *Sci. Total Environ.*, *304*, 61–72.

Feng, X., L. Shang, S. Wang, S. Tang, and W. Zheng (2004a), Temporal variation of total gaseous mercury in the air of Guiyang, China, *J. Geophys. Res.*, *109*, D03303, doi:10.1029/2003JD004159.

Feng, X., H. Yan, S. Wang, G. Qiu, S. Tang, L. Shang, Q. Dai, and Y. Hou (2004b), Seasonal variation of gaseous mercury exchange rate between air and water surface over Baihu reservoir, Guizhou, China, *Atmos. Environ.*, *38*, 4721–4732.

Feng, X., G. Li, and G. Qiu (2004c), A preliminary study on mercury contamination to the environment from artisanal zinc smelting using indigenous method in Hezhang County, Guizhou, China. Part 1: Mercury emission from zinc smelting and its influences on the surface water, *Atmos. Environ.*, *38*, 6223–6230.

Ferrara, R., and B. Mazzolai (1998), A dynamic flux chamber to measure mercury emission from aquatic systems, *Sci. Total Environ.*, *215*, 51–57.

Fitzgerald, W. F., R. P. Mason, and G. M. Vandal (1991), Atmospheric cycling and air-water exchange of mercury over mid-continental lacustrine regions, *Water Air Soil Pollut.*, *56*, 745–767.

Gillis, A., and D. R. Miller (2000), Some potential errors in the measurement of mercury gas exchange at the soil surface using a dynamic flux chamber, *Sci. Total Environ.*, *260*, 181–189.

Gustin, M. S. (2003), Are mercury emissions from geological sources significant? A status report, *Sci. Total Environ.*, *304*, 153–167.

Gustin, M. S., G. E. Taylor, and R. A. Maxey (1997), Effect of temperature and air movement on the flux of element mercury from substrate to atmosphere, *J. Geophys. Res.*, *102*, 3891–3898.

Gustin, M. S., et al. (1999), Nevada STORMS project: Measurement of mercury emissions from naturally enriched surfaces, *J. Geophys. Res.*, *104*, 21,831–21,844.

Gustin, M. S., S. E. Lindberg, K. Austin, M. Coolbaugh, A. Vette, and H. Zhang (2000), Assessing the contribution of natural sources to regional atmospheric mercury budgets, *Sci. Total Environ.*, *259*, 61–71.

Gustin, M. S., H. Biester, and C. S. Kim (2002), Investigation of the light-enhanced emission of mercury from naturally enriched substrate, *Atmos. Environ.*, *36*, 3241–3254.

Hou, Y. (2004), Application of GIS system to study of mercury biogeochemistry in the environment (in Chinese), M.S. thesis, 51 pp., Inst. of Geochem., Chin. Acad. of Sci., Beijing.

Kim, K.-H., S. E. Lindberg, and T. P. Meyers (1995), Micrometeorological measurement of mercury fluxes over background forest soils in eastern Tennessee, *Atmos. Environ.*, *27*, 267–282.

Lamborg, C. H., K. R. Rolfhus, W. F. Fitzgerald, and G. Kim (1999), The atmospheric cycling and air-sea exchange of mercury species in the south and equatorial Atlantic Ocean, *Deep Sea Res., Part II*, *46*, 957–977.

Lamborg, C. H., W. F. Fitzgerald, J. O'Donnell, and T. Torgersen (2002), A non-steady-state compartmental model of global-scale mercury biogeochemistry with interhemispheric atmospheric gradients, *Geochim. Cosmochim. Acta*, *66*, 1105–1118.

Lee, D. S., G. J. Dollard, and S. Pepler (1998), Gas-phase mercury in the atmosphere of the United Kingdom, *Atmos. Environ.*, *32*, 855–864.

Lindberg, S. E., K.-H. Kim, T. P. Meyers, and J. G. Owens (1995), A micrometeorological gradient approach for quantifying air/surface exchange of mercury vapor: Tests over contaminated soils, *Environ. Sci. Technol.*, *29*, 126–135.

Lindberg, S. E., et al. (1999), Increases in mercury emissions from desert soils in response to rainfall and irrigation, *J. Geophys. Res.*, *104*, 21,879–21,888.

Lindberg, S. E., S. Brooks, C.-J. Lin, K. J. Scott, M. S. Landis, R. K. Stevens, M. Goodsite, and A. Richter (2002a), Dynamic oxidation of gaseous mercury in the Arctic troposphere at polar sunrise, *Environ. Sci. Technol.*, *36*, 1245–1256.

Lindberg, S. E., H. Zhang, A. F. Vette, M. S. Gustin, M. O. Barnett, and T. Kuiken (2002b), Dynamic flux chamber measurement of gaseous mercury emission fluxes over soils. Part 2—Effect of flushing flow rate and verification of a two-resistance exchange interface simulation model, *Atmos. Environ.*, *36*, 847–859.

Lindqvist, O., K. Johansson, M. Aastrup, A. Andersson, L. Bringmark, G. Hovsenius, L. Hakanson, and Å. Iverfeldt (1991), Mercury in Swedish environment: Recent research on causes, consequences, and corrective methods, *Water Air Soil Pollut.*, *55*, 23–32.

Mason, R. P., W. F. Fitzgerald, and G. M. Vandal (1992), The sources of mercury in equatorial Pacific rain, *J. Atmos. Chem.*, *14*, 489–500.

Mason, R. P., W. F. Fitzgerald, and F. M. M. Morel (1994), The biogeochemical cycling of elemental mercury—Anthropogenic influences, *Geochim. Cosmochim. Acta*, *58*(15), 3191–3198.

Poissant, L. (2000), Total gaseous mercury in Quebec (Canada) in 1998, *Sci. Total Environ.*, *259*, 191–201.

Poissant, L., and A. Casimir (1998), Water-air and soil-air exchange rate of total gaseous mercury measured at background sites, *Atmos. Environ.*, *32*, 883–893.

Poissant, L., M. Pilote, and A. Casimir (1999), Mercury flux measurements in a naturally enriched area: Correlation with environmental conditions during the Nevada study and tests of release of mercury from soils (STORMS), *J. Geophys. Res.*, *104*, 21,845–21,857.

Rasmussen, P. E., G. C. Edwards, J. Kemp, C. Hubble-Fitzgerald, and W. H. Schroeder (1998), Towards an improved natural sources inventory for mercury, in *Proceedings of Metals and the Environment: An International Symposium*, edited by J. Skeaff, pp. 73–83, Metal. Soc. of the Can. Inst. of Min., Metal. and Pet., Montreal, Quebec, Canada.

Schluter, K. (2000), Review: Evaporation of mercury from soils. An integration and synthesis of current knowledge, *Environ. Geol.*, *39*, 249–271.

Schroeder, W. H., and J. Munthe (1998), Atmospheric mercury: An overview, *Atmos. Environ.*, *32*, 809–822.

Schroeder, W. H., J. Munthe, and O. Lindqvist (1989), Cycling of mercury between water, air and soil compartments of the environment, *Water Air Soil Pollut.*, *48*, 337–347.

Schroeder, W. H., K. G. Anlauf, L. A. Barrie, J. Y. Lu, A. Steffen, D. R. Schneeberger, and T. Berg (1998), Arctic springtime depletion of mercury, *Nature*, *394*, 331–332.

Schroeder, W. H., A. Steffen, G. Lawson, and W. Strachan (2001), Mercury measurements at Alert, in *Synopsis of Research Conducted Under the 2000/2001 Northern Contaminants Program*, edited by S. Kalhok, pp. 130–135, Indian and North. Affairs Can., Ottawa.

Slemr, F., and H. E. Scheel (1998), Trends in atmospheric mercury concentrations at the summit of the Wank Mountain, southern Germany, *Atmos. Environ.*, *32*, 845–853.

Slemr, F., W. Junkermann, R. W. H. Schmidt, and R. Sladkovic (1995), Indication of change in global and regional trends of atmospheric mercury concentrations, *Geophys. Res. Lett.*, *22*, 2143–2146.

Tang, S. (2004), The mercury speciation and emissions from coal combustion and landfill gas in Guiyang (in Chinese), Ph.D. thesis, 85 pp., Inst. of Geochem., Chin. Acad. of Sci., Beijing.

Temme, C., F. Slemr, R. Ebinghaus, and J. W. Einax (2003), Distribution of mercury over the Atlantic Ocean in 1996 and 1999–2001, *Atmos. Environ.*, *37*, 1889–1897.

Urba, A., K. Kvietkus, J. Sakalys, Z. Xiao, and O. Lindqvist (1995), A new sensitive and portable mercury vapor analyzer Gardis-1A, *Water Air Soil Pollut.*, *80*, 1305–1309.

Xiao, Z., J. Munthe, W. H. Schroeder, and O. Lindqvist (1991), Vertical fluxes of volatile mercury over forest soil and lake surfaces in Sweden, *Tellus, Ser. B*, *43*, 267–279.

Zehner, R. E., and M. S. Gustin (2002), Estimation of mercury vapor flux from natural substrate in Nevada, *Environ. Sci. Technol.*, *36*, 4039–4045.

Zhang, H., and S. E. Lindberg (1999), Processes influencing the emission of mercury from soils: A conceptual model, *J. Geophys. Res.*, *104*, 21,889–21,896.

Zhang, H., S. E. Lindberg, M. O. Barnett, A. F. Vette, and M. S. Gustin (2002), Dynamic flux chamber measurement of gaseous mercury emission fluxes over soils. Part 1: Simulation of gaseous mercury emissions from soils using a two-resistance exchange interface model, *Atmos. Environ.*, *36*, 835–846.

X. Feng, Y. Hou, G. Qiu, S. Tang, and S. Wang, State Key Laboratory of Environmental Geochemistry, Institute of Geochemistry, Chinese Academy of Sciences, 46 Guanshui Road, Guiyang 550002, China. (fengxinbin@vip.skleg.cn)

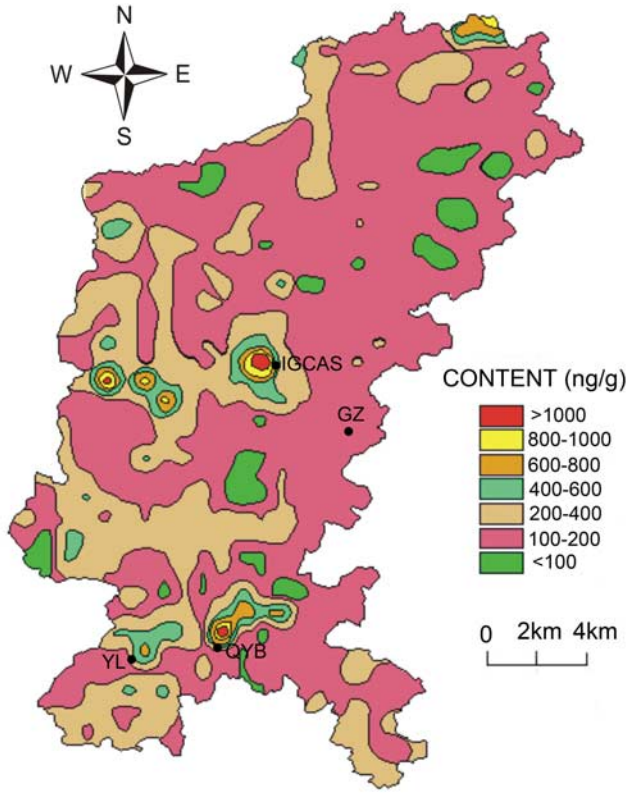


**Figure 3.** Mercury distribution in surficial soil in Guiyang [after *Hou*, 2004].